

Article

Novel Protection Scheme considering Tie Switch Operation in an Open-Loop Distribution System using Wavelet Transform

Hun-Chul Seo 

School of Electronic & Electrical Engineering, Yonam Institute of Technology, Jinju-si, Gyeongsangnam-do 52821, Korea; hunchul0119@hanmail.net or hunchul12@yc.ac.kr; Tel.: +82-55-751-2059

Received: 4 April 2019; Accepted: 3 May 2019; Published: 7 May 2019



Abstract: Loop power distribution systems are gaining increasing attention due to improvements in the reliability of the power supply and the connection of distributed generation. With loop distribution systems, there is the possibility of mal-operation of the protection relay because of the existence of the tie switch and bi-directional current injection. In this paper, we propose a novel protection scheme considering the tie switch operation in the open loop power distribution system using wavelet transform. We analyze the possibility of mal-operation of the protection relay as a result of the normal load current after tie switch operation and analyze the characteristics of the normal load current and fault current injection after tie switch operation. Using these results, a new index is proposed to distinguish the normal load current and fault current, and a novel protection scheme based on this new index is proposed. The proposed method is modeled using an electromagnetic transients program and MATLAB, and the various simulations are performed according to the tie switch position, the fault location, and the success or failure of the fault section separation. From the simulation results, we can confirm that the normal load current and the fault current after tie switch operation can be accurately distinguished and the protection relay can accurately operate at only fault conditions.

Keywords: open loop distribution system; protection scheme; Wavelet Transform; tie switch

1. Introduction

A conventional distribution system is a radial distribution system in which the current flows uni-directionally from the source. Currently, the reliability requirements for electric power supplies are increasing as a result of an increase in sensitive loads and power demands. In addition, the connections of distributed generation (DG) and energy storage systems (ESS) are also increasing. For these reasons, the distribution system is changing from a radial distribution system to a loop distribution system. In a loop power distribution system, a bidirectional power supply is possible, making it possible to minimize the outage and ensure the reliability of the power supply. However, because it is different from conventional radial distribution systems, various problems can occur relating to the system operation, power quality, protection, etc. In view of the power quality, problems such as voltage sags, harmonics reduction, and line losses have been analyzed, and methods for improvement have been proposed [1–4]. Regarding the system operation and configuration, research has been conducted on tie switch connection points, system planning, and locations of DGs for loop system configuration [5–9]. In this paper, we focus on protection issues rather than the abovementioned issues.

In loop power distribution systems, an open-loop/closed-loop distribution system is determined according to the normal open/close of the tie switch. In open-loop distribution systems, the system configuration before closing of the tie switch is the same as the conventional radial distribution

system, and hence the protection method is also the same. However, after closing of the tie switch, there is the possibility of mal-operation of the protection relay related to the current injection from another line. In closed-loop distribution systems, the possibility of mal-operation of the conventional overcurrent relay related to the bidirectional current flow exists. Various studies have been conducted on a protection method in loop distribution systems. In [10], fault location estimation using wavelet transform and support vector machine technology in the loop distribution system was proposed. In [11], a protection technique and a protection coordination method in the loop distribution system with the electric vehicle were analyzed. In [12], the magnitude and direction of the fault current when the wind generator is connected was analyzed and the adaptive relay setting method was proposed. In [13], the problems of the conventional protection scheme in the closed loop power distribution system with DG were analyzed and the pilot protection scheme was proposed. In [14], the optimal configuration method of the DG during recovery after fault occurrence in the loop power distribution system was analyzed. In [15], the protection scheme in a loop-type micro grid was proposed. In [16], the pilot protection scheme in the loop distribution system with a cable was proposed. Some previous works have dealt with protection issues in the closed-loop distribution system. However, these previous works do not analyze the possibility of mal-operation of the protection relay after operation of the tie switch in open-loop distribution systems and so do not propose countermeasures for these problems. As a solution, this paper proposes a novel protection scheme considering tie switch operation in an open-loop distribution system using wavelet transforms (WT). The new contributions of this paper are as follows:

1. The possibility of mal-operation of the protective relay after closing of the tie switch in the open loop distribution system is analyzed.
2. To prevent this mal-operation, a new index to classify the normal load current supply and the fault current injection using the WT is proposed.
3. A novel protection scheme using the new index is proposed.

The remainder of the paper is organized as follows: Section 2 discusses the theory of WTs. Section 3 analyzes the mal-operation of the protection relay after closing of the tie switch in the open-loop distribution system. In Section 4, the characteristics of the normal load current supply and fault current injection after closing of the tie switch are analyzed. In addition, the new index to classify the normal load current supply and the fault current using the WT are proposed. Furthermore, on the basis of this index, a novel protection scheme is proposed. Section 5 discusses the verification of the proposed scheme using an electromagnetic transient program (EMTP) and MATLAB. Finally, the conclusions derived from the study are presented in Section 6.

2. Wavelet Transform

A WT can extract time and frequency information simultaneously from an original signal [17–19]. The discrete wavelet transform (DWT) of a signal is defined as

$$DWT(m, k) = \frac{1}{\sqrt{a_0^m}} \sum_{k=1}^N x(n) g\left(\frac{k - na_0^m b_0}{a_0^m}\right) \quad (1)$$

where $x(n)$ is the input signal, $g(n)$ is the mother wavelet (MW), a_0^m is a scale parameter, $na_0^m b_0$ is the time shift of $g(n)$, and scaling parameter “ a ” and translation parameter “ b ” are functions of integer parameter m [17–19]. The values of a , b , and m are different according to the types of MW.

In general, the low-frequency components of a signal represent its identity and the high-frequency components represent its detailed characteristics. In a WT, these characteristics are defined as approximation (A) and detail (D). In this process, the original signal, S , can be represented as follows [17–19]:

$$S = D_1 + D_2 + \dots + D_n + A_n \quad (2)$$

The DWT can be represented as a tree of low- and high-pass filters, as shown in Figure 1. The output of a high-pass filter provides the detailed information of the high-frequency components of the signal. Moreover, low-frequency components are split further to obtain more details of the input signal. Any wavelet can be implemented using this technique. The original signal is successively decomposed into components of lower resolution, while high-frequency components are not analyzed further. If a WT is used, it is possible to extract the components at any frequency band, and the extracted components can be used to analyze various signals [17–19].

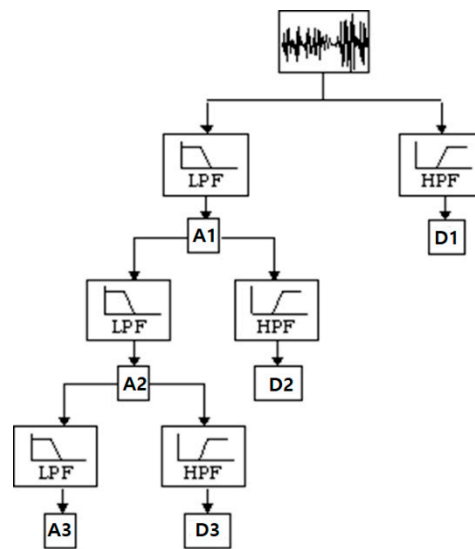


Figure 1. Filter bank representation of the discrete wavelet transform. LPF: Low Pass Filter; HPF: High Pass Filter.

3. Mal-Operation Possibility of Protection Relay according to the Tie Switch Operation in the Open-Loop Distribution System

Figure 2 shows an open loop distribution system in a normal state. Because the tie switch is open, it operates as if the I distribution line and the J distribution line in Figure 2 are separated. Therefore, even if a failure occurs in one line, it does not cause a mal-operation of the protection relay of another line. The problem arises after the fault occurs, the fault section is disconnected, and the tie switch is closed.

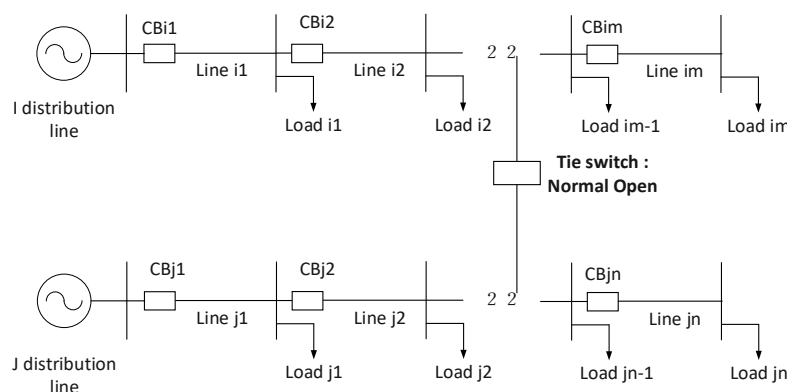


Figure 2. Open loop distribution system.

Figure 3 shows the current flow after a fault has occurred in the I distribution line, the fault section is disconnected, and the tie switch is closed. As shown in Figure 2, if the fault has occurred in Line i1, Line i1 is separated and then the tie switch is closed and the current is supplied to the remaining load of the I distribution line from the J distribution line.

If the line loss is ignored, the currents flowing in the I and J distribution lines in the normal state are

$$I_{Line\ i_steady} = \frac{V_{i1}}{Z_{load_i1}} + \frac{V_{i2}}{Z_{load_i2}} + \dots + \frac{V_{im}}{Z_{load_im}}$$

$$I_{Line\ j_steady} = \frac{V_{j1}}{Z_{load_j1}} + \frac{V_{j2}}{Z_{load_j2}} + \dots + \frac{V_{jn}}{Z_{load_jn}}$$

where, $V_{i1}, V_{i2}, \dots, V_{im}$ are voltage at each bus of the I distribution line in the normal state; $V_{j1}, V_{j2}, \dots, V_{jn}$ are voltage at each bus of the J distribution line in the normal state; $Z_{load_i1}, Z_{load_i2}, \dots, Z_{load_im}$ are impedance of each load of the I distribution line in the normal state; and $Z_{load_j1}, Z_{load_j2}, \dots, Z_{load_jn}$ are impedance of each load of the J distribution line in the normal state.

If the fault occurs in the kth section among the total m sections of I distribution line and the fault section is successfully separated, the current flowing in the J distribution line is expressed by (3).

$$I_{Line\ j_tie} = \frac{V_{j1}}{Z_{load_j1}} + \frac{V_{j2}}{Z_{load_j2}} + \dots + \frac{V_{jn}}{Z_{load_jn}} + \frac{V_{ik}}{Z_{load_{ik+1}}} + \dots + \frac{V_{im}}{Z_{load_im}} \tag{3}$$

The value calculated by (3) is the sum of the load currents from the kth load to mth load at the I distribution line and (2). Therefore, even though it is not a fault, the overcurrent relay (OCR) in the J distribution line has the possibility of mal-operation by detecting the conditions of the instantaneous trip by (4) or the time-inverse trip by (5) depending on the value calculated by (3). If the magnitude of the load current from the k load to the m load is large, the possibility of the mal-operation of the protective relay is also large.

$$I_{Line\ j_tie} \geq k \cdot I_{trip_j} : \text{Instantaneous trip} \tag{4}$$

$$I_{trip_j} \leq I_{Line\ j_tie} < k \cdot I_{trip_j} : \text{Time - inverse trip} \tag{5}$$

where, k is the factor for determination of the instantaneous trip and I_{trip_j} is the minimum trip current.

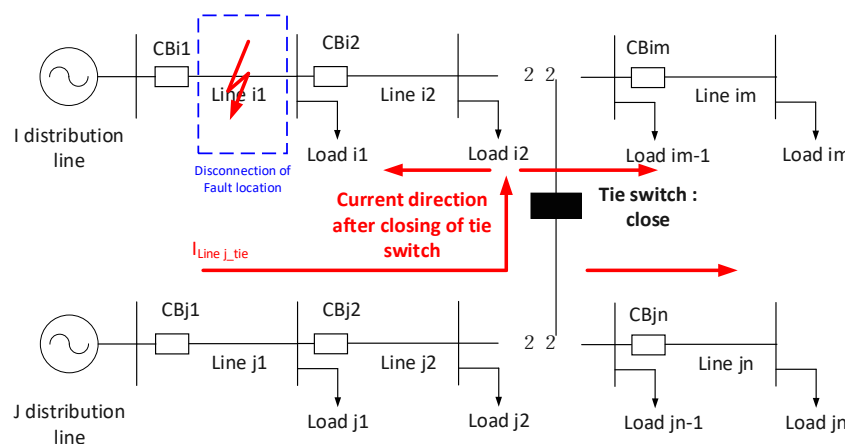


Figure 3. Current flow after the tie switch is closed.

I_{trip_j} may be adjusted to solve the above problem. However, it is very difficult to adjust I_{trip_j} because there is no way to know where the fault occurs. Therefore, there is a difficulty in determining the operation of the protection relay by the magnitude of the current in order to solve this problem. As another countermeasure, even if a directional OCR is used, it is possible to block only a part of the faulted line, blocking in the remaining section cannot be performed, and hence this is not a good solution.

The above problems are relevant to cases where the fault section is successfully separated. We should also consider cases where the tie switch closes even if the fault section separation has

failed. If this happens, it is possible to inject the fault current from the healthy distribution line to the fault section. Therefore, in this case, the protection relay should be operated to interrupt the fault current injection.

4. Novel Protection Scheme using Wavelet Transform in the Open-Loop Distribution System

As described above, there is a possibility of mal-operation of the protection relay related to the operation of the tie switch in the open-loop distribution system. In this case, the protection relay must have the following condition for correct operation: classification of the normal load current supply and fault current injection when the current is injected through the tie switch from the healthy line.

4.1. Characteristics of the Normal Load Current Supply and Fault Current Injection according to the Operation of the Tie Switch in the Open-Loop Distribution System

Figure 4 shows the current flow after the closing of the tie switch when the fault section is successfully disconnected. In the case of Figure 4, because the fault occurs in Line i1, CBI1 and CBI2 are open to separate the fault section. After that, the tie switch is closed and the current from the J distribution line is supplied from Load i2 to Load im. It should be noted that CBI2 is open. A switching surge occurs at the instant when the current begins to flow to the J distribution line after the closing of the tie switch. The switching surge travels along the distribution line. Because the CBI2 is open, the reflected wave is generated at this point, and the reflected current can flow back to the J distribution line. Thereafter, a reflected wave is again generated in a section where the characteristic impedance in the J distribution line is different. After that, a surge current flows to the I distribution line again, and a reflected wave is again generated at the open end. In other words, the flow of current caused by the switching surge shows a form in which (1) and (2) appear repeatedly, as shown in Figure 4. Because the length of the distribution line is short, a switching surge with a high frequency is generated. Furthermore, in the open circuit, because the reflected wave is doubled, the magnitude and duration of the high-frequency switching surge can be prolonged.

Figure 5 shows the current flow after the closing of the tie switch when the fault section is not separated. In the case of the fault being in Line i1, CBI1 normally operates and the fault current injection from the main power is blocked, but CBI2 fails to open and remains closed. If the tie switch is closed without recognizing closed CBI2, the fault current is injected to Line i1 from the J distribution line. The switching surge occurs at an instant when the tie switch is closed. In this case, the reflected wave is generated at the fault point and its magnitude is determined by the fault resistance. However, the size of the reflected wave cannot be larger than that of the open end. In addition, because of the fault current injection, the duration of the high-frequency waveform is very short and decays very quickly.

The differences between Figures 4 and 5 are as follows.

- In the case of Figure 4, the protection relay should not be operated because it is the normal load current supply. However, in the case of Figure 5, the protection relay should be operated because of the fault current injection.
- The high-frequency waveform is generated in Figure 4, however, it is not generated in Figure 5.

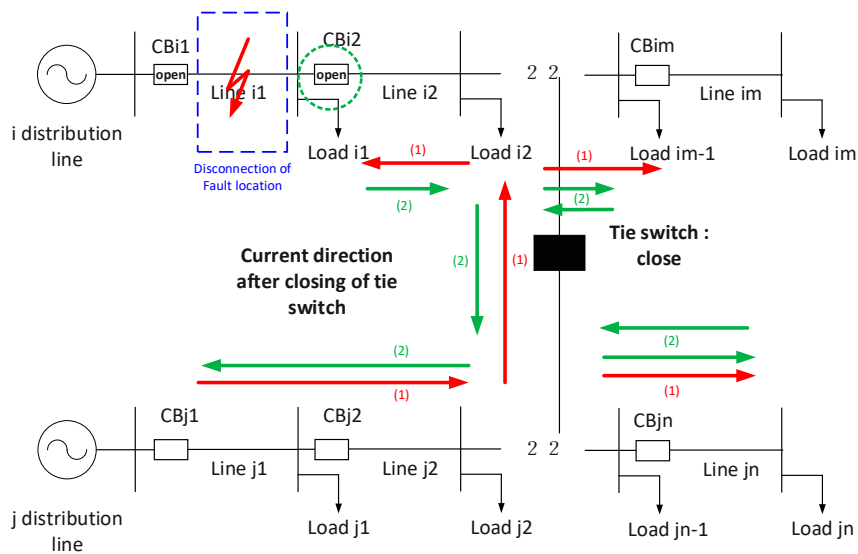


Figure 4. Current flow after the closing of the tie switch when the fault section is successfully disconnected.

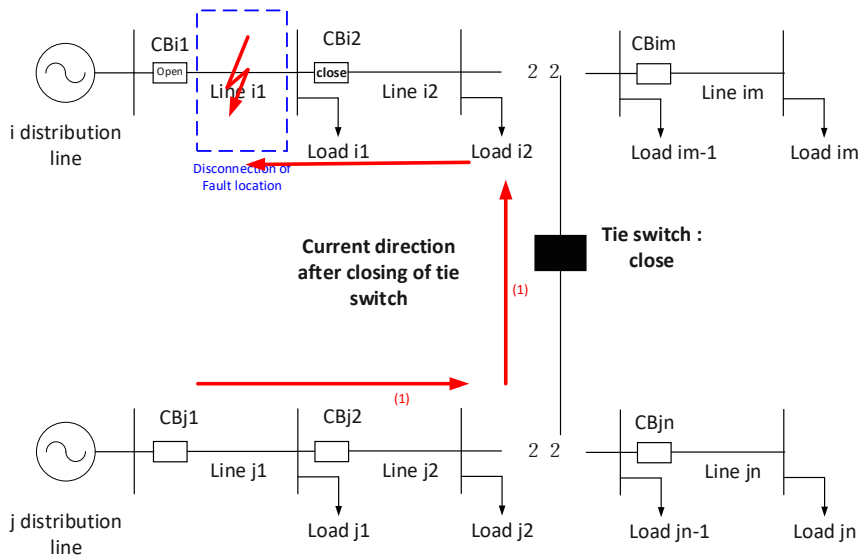


Figure 5. Current flow after the closing of the tie switch when the fault section is unsuccessfully disconnected.

4.2. New Index to Classify the Normal Load Current Supply and Fault Current Injection Using Wavelet Transform

In this paper, we use the switching surge to classify the normal load current supply and fault current injection based on the results of Section 4.1. One of the characteristics of the switching surge is that it contains high frequencies. Therefore, in this paper, we use the WT that can include both time and frequency information to develop a new index for classifying the normal load current and fault current after tie switch operation.

In this paper, the new index in (6) for classifying the normal load current and the fault current is proposed. First, the WT is performed using the current. To utilize the characteristic of having a frequency lower than the normal load current supply in the case of the fault current injection, level 3 is selected (instead of level 1 or 2) which extracts the highest frequency range band. After WT, the level 3 detail coefficient (d3) is used. The d3 coefficient is the value obtained by doubling the decomposition in the WT, as shown in Figure 1. Therefore, it has high-frequency components. The frequency band

of the $d3$ coefficient depends on the types of MW. The proposed new index is the value obtained by taking the absolute value of the $d3$ coefficient and integrating it for one cycle.

$$classification = \int_{t_{present-1cycle}}^{t_{present}} |d3(t)| dt \quad (6)$$

After tie switch operation, the new index value in the fault current injection will have a large value because a waveform with a frequency lower than the normal load current supply is generated. However, in the case of the normal load current supply, the value of the new index will not have a large value.

In a conventional distribution system, the overcurrent relay (OCR) has been used as the primary protection scheme. Therefore, the classical index is only the magnitude of the current. However, in this paper, both the proposed index and the magnitude of the current are used in the proposed protection scheme.

4.3. Selection of Mother Wavelet

There are several types of MWs, including Haar, Daubechies (db) N, Symlets N, Biorthogonal N (Bior N), and Coiflets N (Coif N). MWs can be classified according to their length and characteristics [17–19]. Furthermore, because the wavelets used in signal analysis can be obtained by scaling and shifting the MW, the selection of the MW for classifying the normal load current supply and the fault current injection is very important.

Simulations were performed in a simple distribution system as shown in Figure 6. The distribution lines in Figure 6 were modelled by LINE CONSTANTS in EMTP. The inputs were the radius of line, horizontal length, vertical height, etc. EMTP calculates the resistance and characteristic impedance. Figure 7 shows a configuration of the modeled pole. Figure 8 shows an example of LINE CONSTANTS in EMTP. The distribution lines were modelled using a distributed line model to increase the accuracy of the transient phenomena. The types of overhead distribution line, overhead ground wire, and neutral wire modelled in Figure 6 are the Aluminum Conductor Steel-Reinforced (ACSR) 95 mm², WO 32 mm², and ACSR 60 mm², respectively. The fault occurred in 50% of Line i1. The fault resistance was 1 Ω, and the fault type was a 3 phase-to-ground fault. After the system modeling using EMTP, the current waveform extracted 120 samples per cycle and the WT was performed using MATLAB (R2015a, Mathworks, Natick, MA, USA). We compared haar, db4, sym5, bior 3.1, and coif4, which are the most commonly used in power system signal analysis, to select the MW.

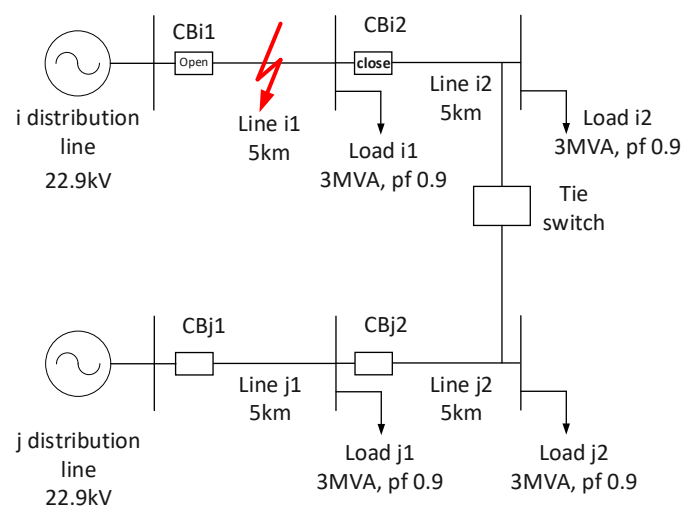


Figure 6. Simple distribution system.

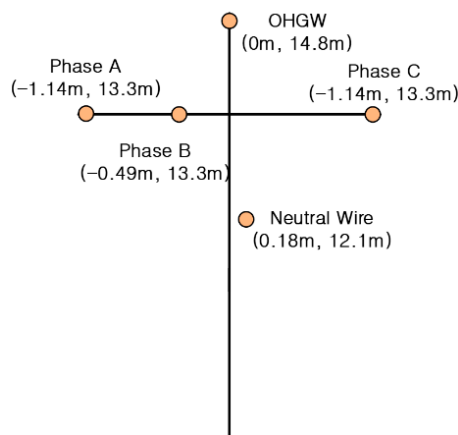


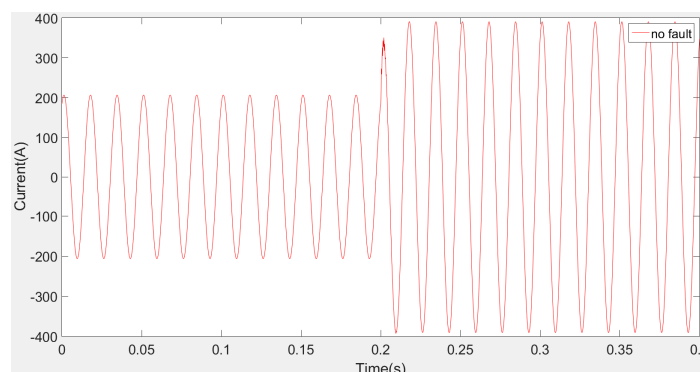
Figure 7. Configuration of modelled pole.

Line/Cable Data: 3

#	Ph.no.	Rin [cm]	Rout [cm]	Resis [ohm/km DC]	Horiz [m]	Vtower [m]	Vmid [m]
1	1	0.39	0.91	0.182	-1.14	11	11
2	2	0.39	0.91	0.182	-0.49	11	11
3	3	0.39	0.91	0.182	1.14	11	11
4	4	0.13	0.39	0.898	0	13.475	13.475
5	5	0.225	0.675	0.301	0	9.8	9.8

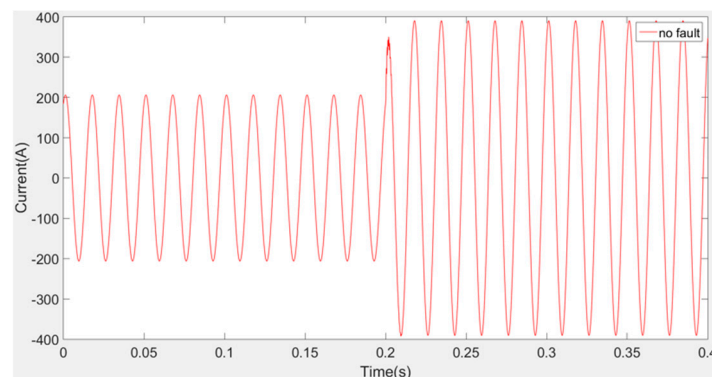
Figure 8. Example of LINE CONSTANTS in the electromagnetic transient program (EMTP).

Figure 9 shows the current waveform measured at CBj2 in Figure 6. In Figure 9a, no fault means that the normal load current was supplied as a result of the success of the fault section separation. In Figure 9b, the fault means that the fault current was introduced because of the failure of the fault section separation. The WT was performed using this current.



(a)

Figure 9. Cont.



(b)

Figure 9. Current waveform measured at CBj2. (a) Current waveform at no fault condition; (b) Current waveform at fault condition.

Figures 10–14 shows the calculation results of the d3 coefficient and the new index proposed in (6) using haar, db4, sym5, bior3.1, and coif4 as MW. In each figure, the meaning of no fault and fault is the same as in Figure 9. The maximum value of no fault and fault and the time required to reach the maximum value were compared to extract the most appropriate MW. The comparison results are shown in Table 1.

Table 1. Comparison of simulation results. MW = mother wavelet.

MW	Maximum Value			Time Required to Reach the Maximum Value	
	Fault	No Fault	Difference	Fault (s)	No Fault (s)
Haar	15220	3190	12030	0.2165	0.0165
Db4	392.5	57.2	335.3	0.2134	0.0134
Sym5	574.9	121.3	453.6	0.2132	0.0132
Bior3.1	953.3	122	831.3	0.2145	0.0145
Coif4	694.3	109.4	584.9	0.2095	0.0095

In Table 1, the largest difference between the maximum values of no fault and fault are presented in haar, followed by bior 3.1, coif4, sym5, and db4. The time to reach the maximum value was fastest for coif4, followed by sym5, db4, bior 3.1, and haar. Although the difference between the fault and the no fault was greatest for the haar MW, the time to reach the maximum value was the slowest for haar, so haar was excluded from the selection of the MW. In addition, db4, which had the smallest difference between the no fault and the fault, was also excluded from the selection of the MW. Among the remaining three MWs, the difference in value was greatest for bior 3.1, but the time to reach the maximum value was slow. In Sym 5, the difference was smaller than in coif 4, and the time to reach the maximum value was also slow. In the case of coif4, the time to reach the maximum value was the fastest, and the difference between the fault and no fault was large (above 550), so we decided to select the coif4 as the MW.

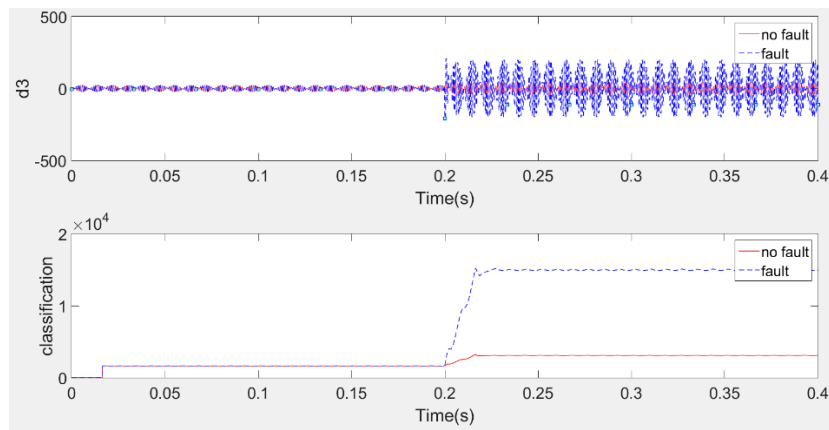


Figure 10. D3 coefficient and new index at haar MW.

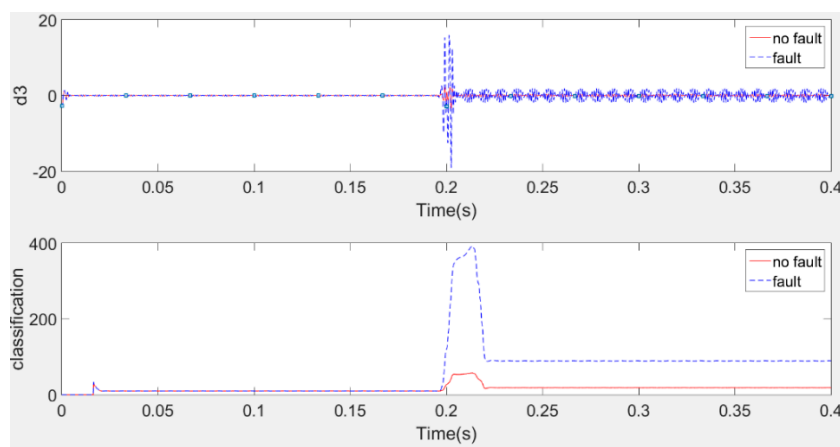


Figure 11. D3 coefficient and new index at db4 MW.

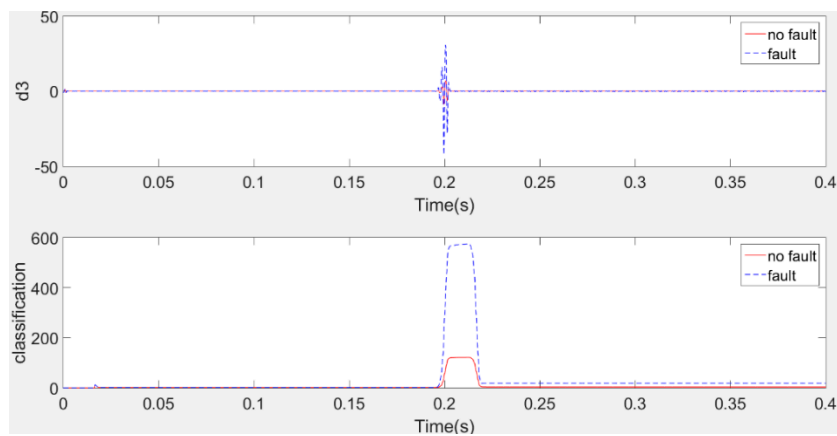


Figure 12. D3 coefficient and new index at sym5 MW.

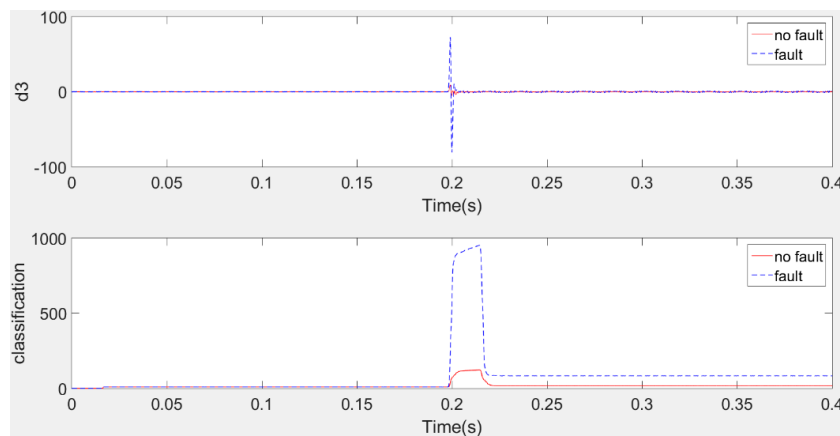


Figure 13. D3 coefficient and new index at bior3.1 MW.

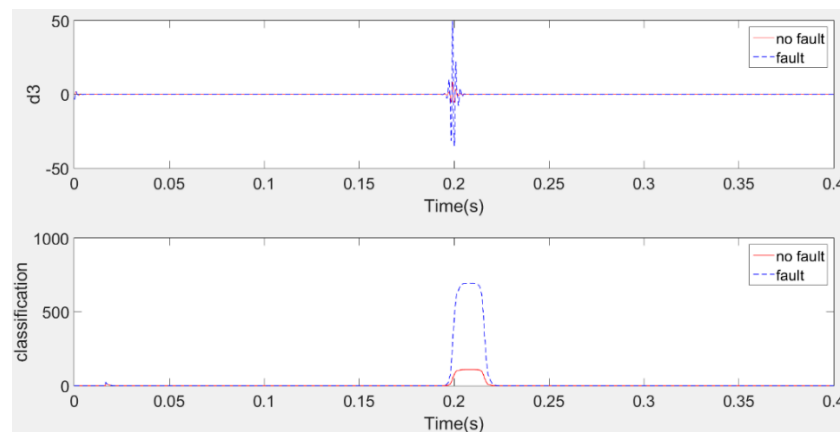


Figure 14. D3 coefficient and new index at coif4 MW.

4.4. Protection Scheme using Wavelet Transform in an Open Loop Distribution System

Figure 15 shows the flowchart of the protection scheme considering the tie switch operation in the open-loop distribution system using the WT. First, the line current is inputted, and the WT is performed using this current. The MW is coif4 as determined in Section 4.3. At the same time, the root mean square (rms) value of the current is calculated. For the next step, the classification proposed in (6) is calculated. If the rms value of the current is larger than the minimum trip current (I_{trip}) and the classification is larger than α , the judge is increased as the number one in order to judge the fault occurrence. If the judge is larger than β , it has detected that the fault has occurred. Thereafter, if the current time exceeds the trip time of the OCR, the protection relay operates normally. α is the threshold value to distinguish the normal load current supply and fault current injection. β is the duration to determine the fault occurrence.

If the rms value of the current is larger than the minimum trip current but the classification is less than α , then it is determined as the normal load current supply and the blocking signal is transmitted to the protection relay. Of course, if the rms value of the current is less than the minimum trip current, the protection relay will not operate.

The advantages of the proposed protection scheme are as follows.

- No additional communication facilities are required among fault lines, tie switches, and healthy distribution lines.
- The nature functions of the OCR are also included, so that it can be operated correctly regardless of the fault locations.

Transients in the distribution line are very fast. This transient phenomenon is caused by the traveling wave after the tie switch is closed. In addition, protection methods using the traveling wave in the distribution system have been studied by several researchers [20–25]. In this paper, the new protection scheme is proposed based on the transient phenomena by the traveling wave. The proposed method extracts 120 samples/cycle. Therefore, the proposed method uses the specific samples, and so it has good accuracy despite the perturbation in the distribution system being fast.

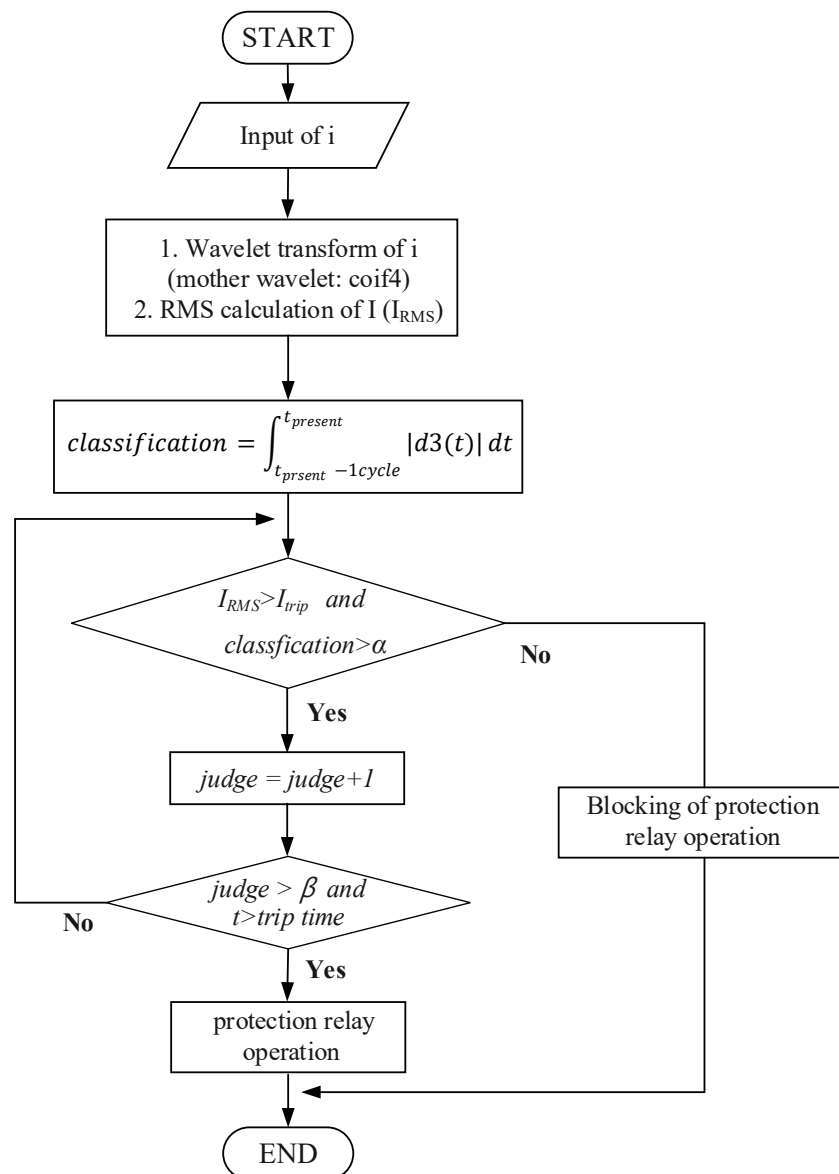


Figure 15. Flow chart of protection scheme using wavelet transform in open loop distribution system. RMS: root mean square.

5. Simulations

5.1. System Model

The proposed protection scheme was verified using the actual distribution system model of Korea Electric Power Corporation, as shown in Figure 16. The two X and Y distribution lines were connected by a tie switch. The connection points of the tie switch were assumed to be the middle part of the system (tie switch (1)) and the end part (tie switch (2)), as shown in Figure 14. In the X distribution line and the Y distribution line, all distribution lines were modelled as distributed line models by the LINE CONSTANTS of EMTP. The geometrical configuration of the distribution pole is presented in Figure 7. The line type and length of each line are shown in Figure 16. The load capacity is also presented in Figure 16. All loads in Figure 16 have a power factor of 0.9. The system model is modeled using EMTP.

5.2. Simulation Conditions

The simulation conditions used to verify the proposed protection scheme are shown in Table 2. The various simulations were performed according to the tie switch position, the fault location, and the success or failure of fault section separation. The tie switch positions were the middle part of the system (tie switch (1)) and the end part (tie switch (2)). The fault locations occurred at a far point from the tie switch and at a nearby point. When the tie switch position was tie switch (1), in Figure 16, 102 sections (cases 1 and 2) and 105 sections (cases 3 and 4) were selected as the fault locations. If the tie switch position was tie switch (2), the simulation was performed by selecting 102 sections (cases 5 and 6) and 107 sections (cases 7 and 8). In addition, the simulations were also performed for both success and failure of the fault section separation. A total eight cases were simulated.

Table 2. Simulation conditions.

Case	Tie Switch Position	Fault Location at X Distribution Line	Fault Section Separation
Case 1	Tie switch (1)	102 section	Success
Case 2	Tie switch (1)	102 section	Failure
Case 3	Tie switch (1)	105 section	Success
Case 4	Tie switch (1)	105 section	Failure
Case 5	Tie switch (2)	102 section	Success
Case 6	Tie switch (2)	102 section	Failure
Case 7	Tie switch (2)	107 section	Success
Case 8	Tie switch (2)	107 section	Failure

The fault type was a single line-to-ground fault and the fault resistance was 1 Ω . The fault occurred at 0.1 s and the protection relay in the X distribution system operated at 0.15 s. The tie switch was closed at 0.2 s. We simulated each case using EMTP and extracted 120 samples per cycle. Using these data, the WT was performed using MATLAB. In addition, the proposed protection scheme was implemented using MATLAB and the protection relay operation was determined. The breaker open/close time was set as three cycles. Furthermore, α and β were set to 1000 and 40, respectively. The minimum trip current was set at 1.5 times of the normal current.

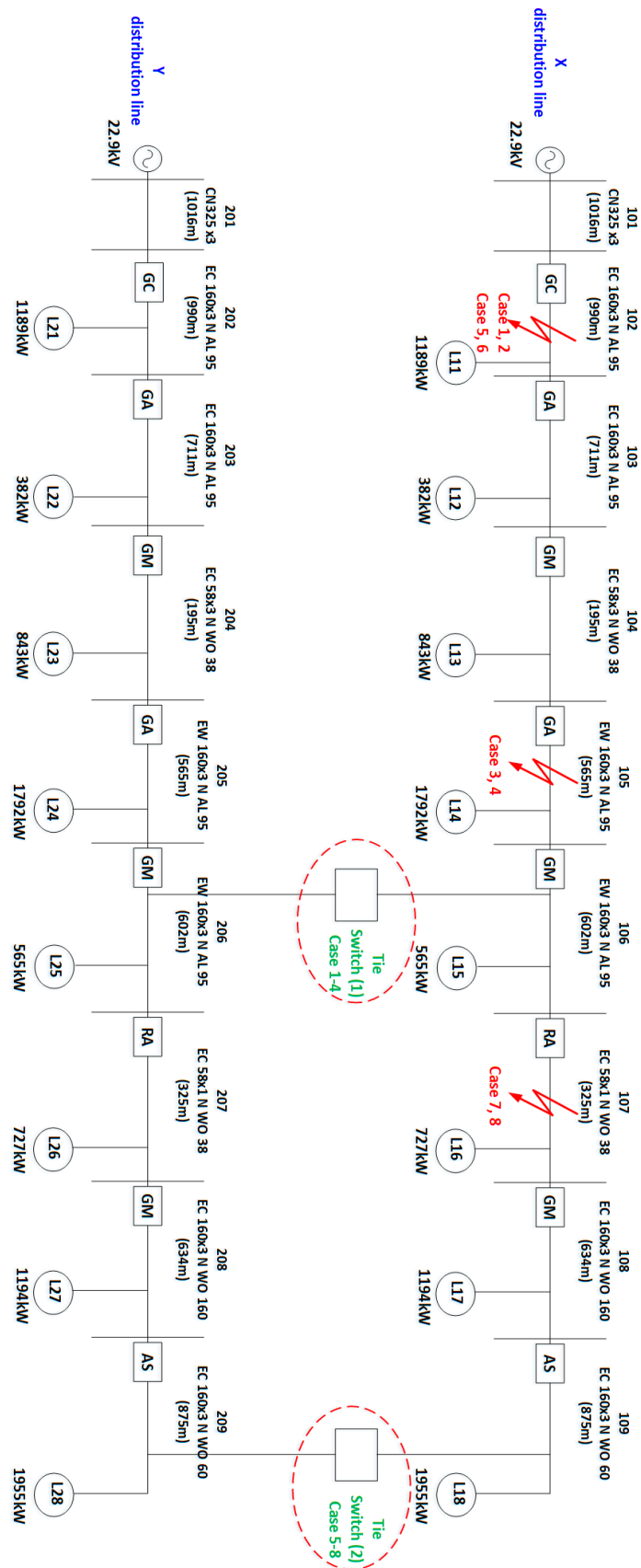


Figure 16. Actual Korea Electric Power Corporation distribution system model.

5.3. Simulation Results and Discussion

In the simulation results, we compared the proposed protection scheme and the conventional OCR. In each Figure, “proposed” means the results of the proposed protection scheme and “conventional” means the results when the conventional OCR was applied as a protection relay.

Figure 17 shows the simulation results of case 1 and case 2. Figure 17a shows the calculation result of the classification proposed in (6). The classification value in case 2 sharply increased beyond α after closing of the tie switch. However, this value did not increase in case 1, which was the case of successful fault section separation. Figure 17b shows the relay trip signal. Here, 1 means breaker close command and 0 means open state. In case 2, because the classification value increased more than α due to the fault and the current was larger than the minimum trip current, the trip command was generated at 0.206 s. Figure 17c shows the current flowing in case 1. The maximum current value of 45 A was flowing before 0.2 s. After the tie switch was closed, this current increased to over double, which satisfied the trip condition of the OCR. Therefore, as shown in Figure 17c, the current became zero as a result of the OCR. The loads experienced an outage although the fault did not occur in the Y distribution line. However, according to the protection scheme proposed in this paper, the normal load current was continuously supplied without the protection relay operation. In Figure 17d, the trip command was generated at 0.206 s because of the fault, and the current after the breaker operation (three cycles) became zero. In case 2, the proposed and conventional results were the same because the two methods were operated to prevent the fault current injection. Figure 18 shows the simulation results of cases 3 and 4. As shown in Figure 18a, the tie switch was closed at 0.2 s, the calculation result of classification value increases sharply beyond α in case 4, but this value did not increase in case 3. Therefore, as shown in Figure 18b, in case 4, the breaker trip command occurred at 0.2056 s. Figure 18c shows the current flowing in the Y distribution line in case 3. After the tie switch closed, the maximum value of current increased rapidly, more than doubling. In the conventional OCR, the trip condition was satisfied and the relay generated the trip signal. Therefore, the current became zero. However, in the proposed protection scheme, the classification value did not increase above α as shown in Figure 18a, hence the trip command did not occur as shown in Figure 18b. Therefore, the normal current was continuously supplied to the loads. Figure 18d shows the current flowing in the Y distribution line in case 4. Since it is the situation of the fault current injection, the trip command was generated at 0.2056 s and the current was cut off completely in 0.2556 s after the breaker operation.

Figure 19 shows the simulation results of cases 5 and 6. As can be seen in Figure 19a, the classification value did not increase in case 5 after the tie switch was closed, but in case 6, it increased sharply above the set value. Therefore, in case 6, the trip signal was generated at 0.206 s as shown in Figure 19b. Figure 19c,d show the currents flow in the Y distribution line in cases 5 and 6. The current was measured at the end of the system to which the tie switch was connected. Therefore, the value of the steady-state current was smaller than that of Figures 17 and 18. Figure 19c shows that after the tie switch was closed at 0.2 s, the maximum value of 20 A increased 4.5 times more than 90 A. In the conventional OCR, the instantaneous trip condition was satisfied. Therefore, as shown in Figure 19c, the current in the conventional OCR became zero and the loads experienced the outage. However, in the proposed protection scheme, the classification value did not increase above α , as shown in Figure 19a. Therefore, as shown in Figure 19b, the trip signal did not occur in case 5. Therefore, the current in case 5 was continuously supplied to the loads. However, in case 6, a trip command was generated and the current was completely shut off after the circuit breaker operation, as shown in Figure 19d.

Figure 20 shows the simulation results of cases 7 and 8. The results are very similar to those in Figure 19. In Figure 20c, three times more current than that of the steady current was flowing after the tie switch closed, however, case 7 was the case of the normal current supply not the fault. Therefore, the classification value did not increase above α , as shown in Figure 20a, and the trip command did not occur, as shown in Figure 20b. In case 8, as shown in Figure 20a, since the classification value increased rapidly after the tie switch closed, a trip command occurred, as shown in Figure 20b and the current

was completely cut off, as shown in Figure 20d. The results in cases 7 and 8 were very similar with other cases. In case 7, when the proposed scheme was applied, the load did not experience the outage. However, in the conventional OCR, the load experienced the outage. In Figure 20d, the results were the same because of the situation of the fault current injection.

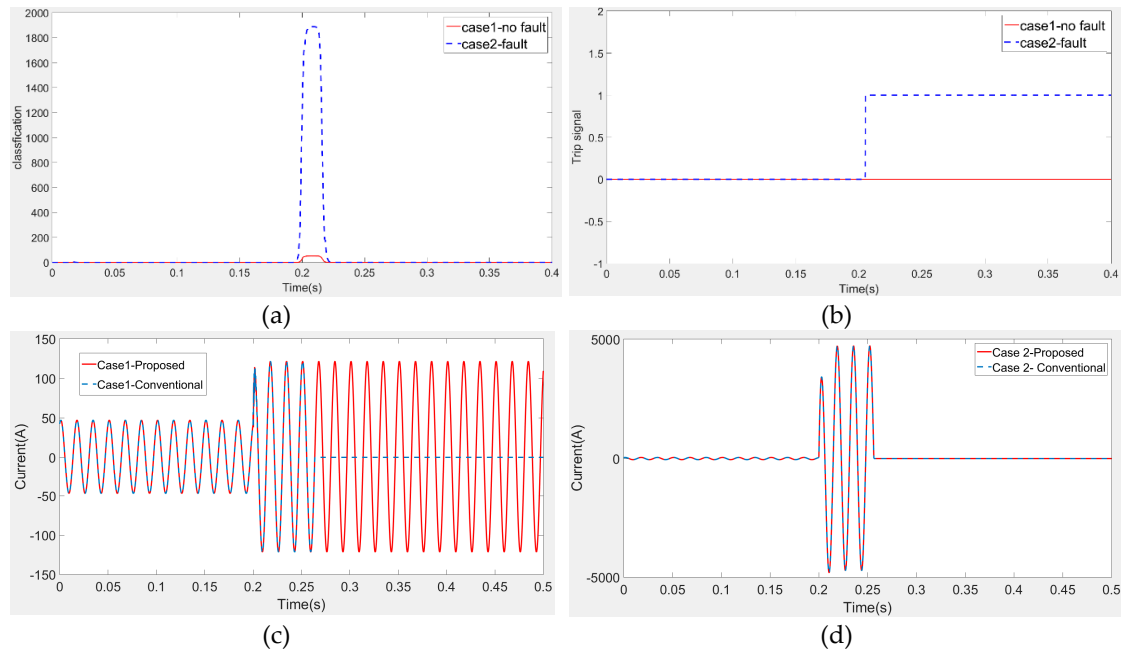


Figure 17. Simulation results of case 1 and 2. (a) Calculation result of classification value; (b) Trip signal; (c) Current flowing in the Y line in case 1; (d) Current flowing in the Y line in case 2.

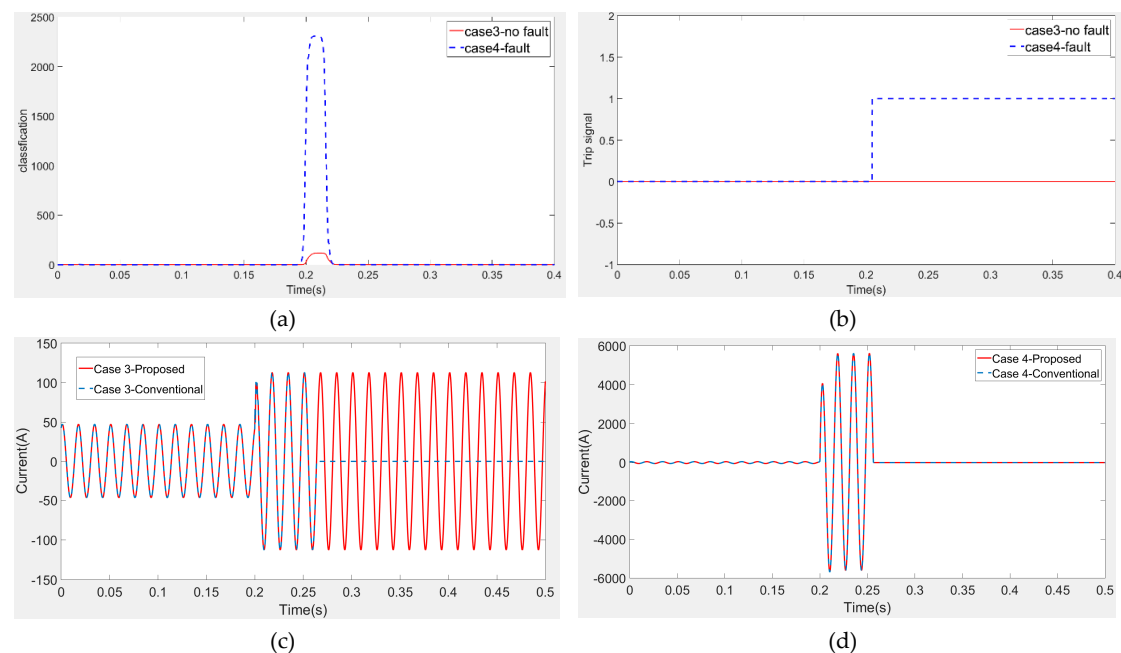


Figure 18. Simulation results of case 3 and 4. (a) Calculation result of classification value; (b) Trip signal; (c) Current flowing in the Y line in case 3; (d) Current flowing in the Y line in case 4.

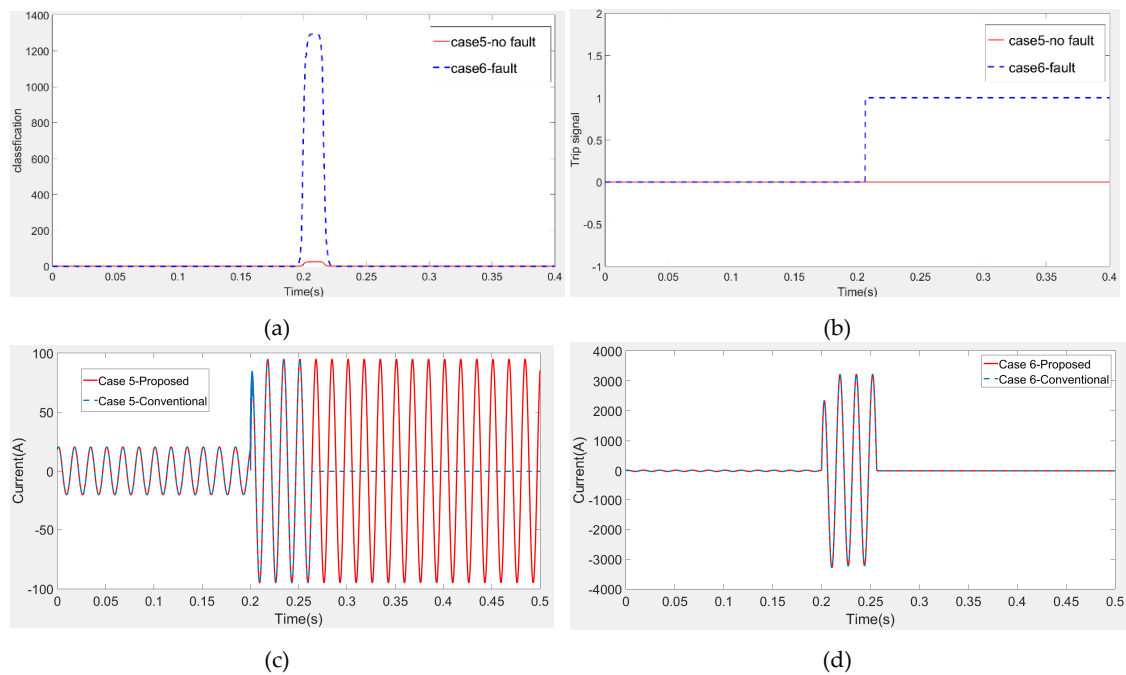


Figure 19. Simulation results of case 5 and 6. (a) Calculation result of classification value; (b) Trip signal; (c) Current flowing in the Y line in case 5; (d) Current flowing in the Y line in case 6.

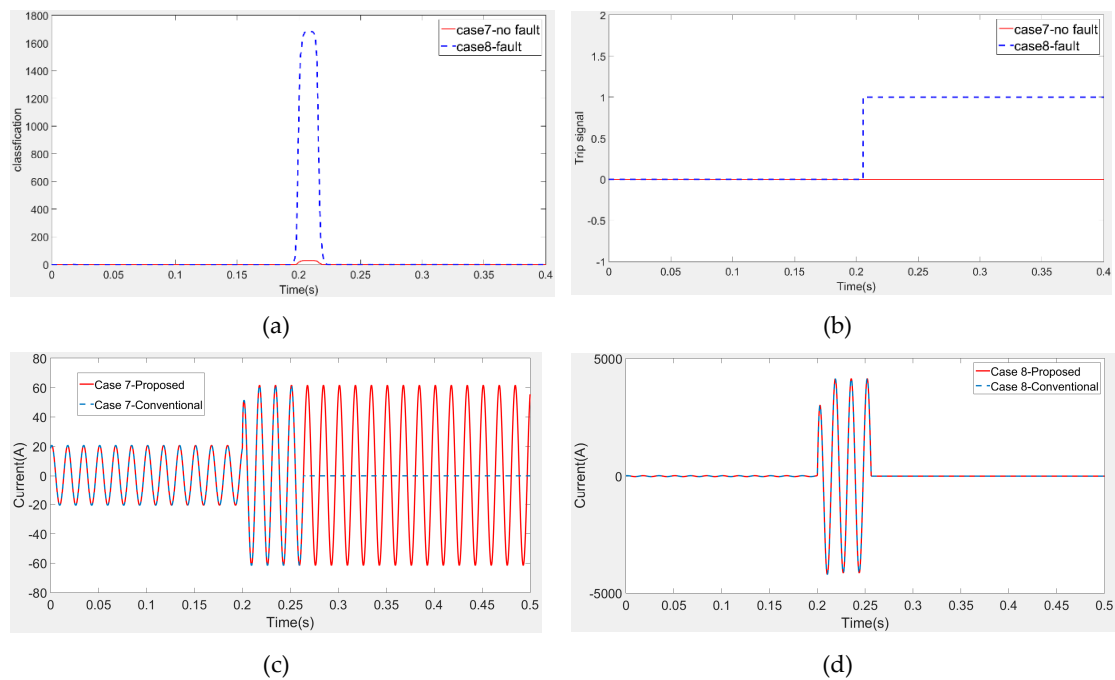


Figure 20. Simulation results of case 7 and 8. (a) Calculation result of classification value; (b) Trip signal; (c) Current flowing in the Y line in case 7; (d) Current flowing in the Y line in case 8.

6. Conclusions

Distribution systems are changing from conventional radial systems to loop systems due to the sudden increase in the load, the connection of the DG, and the reliability requirements associated with an increase of the power supply. In loop distribution systems, there is a possibility of mal-operation of the protection relay because of the tie switch operation. In this paper, we proposed a novel protection scheme.

In this paper, firstly, the reason for the possible mal-operation of the protection relay attributable to the additional load current supply after the tie switch operation in the loop distribution system was analyzed. To solve this problem, we analyzed the characteristics of the normal load current supply and the fault current injection after tie switch closure. On this basis, we proposed a new index to classify the normal load current supply and the fault current injection using WT. The coil4 MW was selected based on the simulation results in the simple distribution system. We proposed a novel protection scheme using the proposed index. The proposed protection scheme can accurately classify the normal load current supply and the fault current injection and can generate a trip command under only fault conditions.

The proposed protection scheme was verified using the actual distribution system. The simulations were performed by changing the tie switch position, the fault location, and the success/failure of the fault section separation. It was found that the load current could be continuously supplied without tripping using the protection scheme proposed in this paper even with currents that doubled after the tie switch closed. In addition, it was found that when the fault current was injected as a result of failure of the fault section separation, the protection relay could be operated normally.

The disadvantage of the proposed protection scheme is that the healthy line is tripped after the tie switch is closed in case of a failure of fault section separation. As a future study, we will investigate the protection scheme using coordination between the tie switch and the protection relay by applying the fault location. Furthermore, we will develop a new protection scheme considering the connections of distributed generation and an energy storage system.

Funding: This research received no external funding.

Conflicts of Interest: The authors declare no conflict of interest

References

1. Moon, J.-F.; Kim, J.-S. Voltage Sag Analysis in Loop Power Distribution System With SFCL. *IEEE Trans. Appl. Supercond.* **2013**, *23*. [[CrossRef](#)]
2. Sayed, M.A.; Takeshita, T. Line Loss Minimization in Isolated Substations and Multiple Loop Distribution Systems Using the UPFC. *IEEE Trans. Power Electron.* **2014**, *29*, 5813–5822. [[CrossRef](#)]
3. Lee, T.-L.; Hu, S.-H. Discrete Frequency-Tuning Active Filter to Suppress Harmonic Resonances of Closed-Loop Distribution Power Systems. *IEEE Trans. Power Electron.* **2011**, *26*, 137–148.
4. Sun, X.; Yang, L.; Wang, R.; Han, R.; Shen, H.; Chen, Z. A Novel Impedance Converter for Harmonic Damping in Loop Power Distribution Systems. *IEEE J. Emerg. Sel. Top. Power Electron.* **2016**, *4*, 162–173. [[CrossRef](#)]
5. Nagata, T.; Okuda, H.; Yamamura, N.; Ueda, F. The Study Related to Searching Method Optimal Connecting Point on Multi-Loop Power Distribution System. In Proceedings of the International Conference on Electrical Machines and Systems, Jeju, Korea, 7–10 October 2018.
6. Che, L.; Zhang, X.; Shahidehpour, M.; Alabdulwahab, A.; Yusuf, A.-T. Optimal Planning of Loop-Based Microgrid Topology. *IEEE Trans. Smart Grid* **2017**, *8*, 1771–1781. [[CrossRef](#)]
7. Ahmed, A.H.; Hasan, S. Optimal allocation of distributed generation units for converting conventional radial distribution system to loop using particle swarm optimization. *Energy proced.* **2018**, *153*, 118–124. [[CrossRef](#)]
8. Javaid, B.; Arshad, M.A.; Ahmad, S.; Kazmi, S.A.A. Comparison of Different Multi Criteria Decision Analysis Techniques for Performance Evaluation of Loop Configured Micro Grid. In Proceedings of the International Conference on Computing, Sindh, Pakistan, 30–31 January 2019.
9. Liu, J.; Cheng, H.; Tian, Y.; Yao, L. An Optimal N-1 Secure Operation Mode for Medium-voltage Loop Distribution Networks Considering Load Supply Capability and Security Distance. *Electr. Power Compon. Syst.* **2017**, *45*, 1393–1403. [[CrossRef](#)]
10. Deng, X.; Yuan, R.; Xiao, Z.; Li, T.; Wang, K.L.L. Fault location in loop distribution network using SVM technology. *Int. J. Electr. Power Energy Syst.* **2015**, *65*, 254–261. [[CrossRef](#)]
11. Lazarou, S.; Vita, V.; Ekonomou, L. Protection Schemes of Meshed Distribution Networks for Smart Grids and Electric vehicles. *Energies* **2018**, *11*, 3106. [[CrossRef](#)]

12. Hsieh, S.-C.; Chen, C.-S.; Tsai, C.-T.; Hsu, C.-T.; Lin, C.-H. Adaptive Relay Setting for Distribution Systems Considering Operation Scenarios of Wind Generators. *IEEE Trans. Ind. Appl.* **2014**, *50*, 1356–1363. [[CrossRef](#)]
13. Li, B.; Yu, X.; Bo, Z. Protection Schemes for Closed loop Distribution Network with Distributed Generator. In Proceedings of the International Conference on Sustainable Power Generation and Supply, Nanjing, China, 6–7 April 2009.
14. Hamad, A.-E.F.; Abd el-Ghany, H.A.; Azmy, A.M. Switching strategy for DG optimal allocation during repairing fault periods on loop distribution networks. *Int. Trans. Electr. Energy Syst.* **2017**, *27*. [[CrossRef](#)]
15. Liu, X.; Shahidehpour, M.; Li, Z.; Liu, X.; Cao, Y.; Tian, W. Protection Scheme for Loop-Based Microgrids. *IEEE Trans. Smart Grid* **2017**, *8*, 1340–1349. [[CrossRef](#)]
16. Tian, Y.; Zhao, Q.; Zhang, Z.; Li, L.; Crossley, P. Current-phase-comparison-based pilot protection for normally closed-loop distribution network with underground cable. *Int. Trans. Electr. Energy Syst.* **2019**, *29*, e2733. [[CrossRef](#)]
17. Park, J.-H.; Seo, H.-C.; Kim, C.-H.; Rhee, S.-B. Development of adaptive reclosing scheme using wavelet transform of neutral line current in distribution system. *Electr. Power Compon. Syst.* **2016**, *44*, 426–433. [[CrossRef](#)]
18. Lee, J.-W.; Kim, W.-K.; Oh, Y.-S.; Seo, H.-C.; Jang, W.-H.; Kim, Y.S.; Park, C.-W.; Kim, C.-H. Algorithm for fault detection and classification using wavelet singular value decomposition for wide-area protection. *J. Electr. Eng. Technol.* **2015**, *10*, 729–739. [[CrossRef](#)]
19. Seo, H.-C.; Rhee, S.-B. Novel adaptive reclosing scheme using wavelet transform in distribution system with battery energy storage system. *Int. J. Electr. Power Energy Syst.* **2018**, *97*, 186–200. [[CrossRef](#)]
20. Dong, X.; Wang, J.; Shi, S.; Wang, B.; Dominik, B.; Redefern, M. Traveling wave based single-phase-to-ground protection method for power distribution system. *CSEE J. Power Energy Syst.* **2015**, *1*, 75–82. [[CrossRef](#)]
21. Li, X.; Dyśko, A.; Burt, G.M. Traveling Wave-Based Protection Scheme for Inverter-Dominated Microgrid Using Mathematical Morphology. *IEEE Trans. Smart Grid* **2014**, *5*, 2211–2218. [[CrossRef](#)]
22. Magnago, F.H.; Abur, A. A New Fault Location Technique for Radial Distribution Systems Based on High Frequency Signals. In Proceedings of the IEEE Power Engineering Society Summer Meeting, Edmonton, Canada, 18–22 July 1999.
23. Kojovic, L.A.; Esztergalyos, J. Traveling Wave Based Relay Protection. United States Patents US7973536B2, 5 July 2011.
24. Zeng, X.; Li, K.K.; Liu, Z.; Yin, X. Fault Location Using Traveling Wave for Power Networks. In Proceedings of the IEEE Industry Applications Conference, Seattle, DC, USA, 3–7 October 2004.
25. Davydova, N.; Hug, G. Traveling Wave Based Protection for Medium Voltage Grids with Distributed Generation. In Proceedings of the IEEE Manchester PowerTech, Manchester, UK, 18–22 June 2017.



© 2019 by the author. Licensee MDPI, Basel, Switzerland. This article is an open access article distributed under the terms and conditions of the Creative Commons Attribution (CC BY) license (<http://creativecommons.org/licenses/by/4.0/>).